PROPAGATION REGIME OF IRON DUST FLAMES

François-David Tang[1], Samuel Goroshin[2], Andrew J. Higgins[2]

[1]European Space Agency, ESTEC; Kaplerlaan 1, Noordwijk, The Netherlands
[2]McGill University, Department of Mechanical Engineering
817 Sherbrooke St. West, Montreal, Quebec, Canada

Keywords: Iron powder, Combustion, Reduced gravity

Abstract

A flame propagating through an iron-dust mixture can propagate in two asymptotic regimes. When the characteristic time of heat transfer between particles is much smaller than the characteristic time of particle combustion, the flame propagates in the continuum regime where the heat released by reacting particles can be modelled as a space-averaged function. In contrast, when the characteristic time of heat transfer is much larger than the particle reaction time, the flame can no longer be treated as a continuum due to dominating effects associated with the discrete nature of the particle reaction. The discrete regime is characterized by weak dependence of the flame speed on the oxygen concentration compared to the continuum regime. The discrete regime is observed in flames propagating through an iron dust cloud within a gas mixture containing xenon, while the continuum regime is obtained when xenon is substituted with helium.

Introduction

While the combustion of powdered metals is typically associated in solid-fueled rockets, metallic fuels have recently been suggested as a potential energy carrier for transport vehicles as a sustainable alternative to fossil fuels [1]. To exploit these applications, a fundamental understanding of the metallic dust flames is essential, but experimental results on fundamental flame parameters are scarce. As a result, current models of laminar flames propagating in heterogeneous media are simply based on a continuum assumption, which underlines the fact that the interparticle spacing l_p is much smaller than the flame width l_d. This assumption permits the function describing the heat release in the reaction zone to be described as a continuous function in space and the governing equations to be expressed as a set of partial differential equations [2,3].

However, if the interparticle distance l_p is on the same order of magnitude as the flame width l_d, then the continuum fails to describe the propagation of the flame. The flame exhibits so-called discrete characteristics where the propagation of the front is dominated by local ignition interactions between neighboring particles. The heat release function becomes dependent on the spatial distribution of the particles and the flame can no longer be described by the continuum theory [4,5]. The parameter quantifying the regime of propagation is the dimensionless combustion time defined as:

$$\tau_c = \frac{t_r \alpha}{l^2}, \qquad (1)$$

where t_r is the characteristic particle reaction time, α is the thermal diffusivity of the gas mixture and l is the interparticle spacing. The discrete regime is realized when $\tau_c < 1$, while the continuum is when for $\tau_c \gg 1$ [5].

In this work, the discrete regime is realized in an experiment where flames propagating through clouds of iron particulates are observed in low-thermal diffusivity, oxidizing environment, namely xenon-oxygen. In contrast, the continuum regime is achieved in a helium-oxygen mixture, which is characterized by a high thermal diffusivity. The continuum and discrete regimes are differentiated using the response of the flame speed to variations of the oxygen concentration.

Experimental Details

The dust combustion experiment uses a flame in an open-ended tube methodology that allows observation of a constant-pressure laminar flame. Experiments were performed onboard a reduced-gravity parabolic flight aircraft to minimize particle settling and buoyancy-induced convective flows. The schematics of the apparatus are shown in Fig. 1.

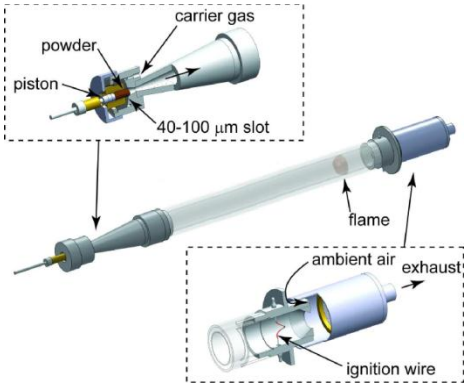

Figure 1: Schematic of the dust combustion experiment. The top left inset illustrates the design of the dust dispersion system and the bottom right inset the design of the first stage cooling and filtering systems.

The powder dispersion unit (see top inset in Fig. 1) consists of a dust feeder and a disperser. The initially compacted dust is fed via a small syringe-type device. As it is fed by the piston, the dust column is continuously dispersed via the impact of a transverse sonic gas jet produced by a 40-100 μm circular slot at the base of the conical dispersion chamber (see top inset in Fig. 1). The conical diffuser connecting the dust dispersion unit with the combustion tube provides expansion and laminarization of the initially highly turbulent flow containing the dispersed dust. The combustion tube is a Pyrex glass tube with an internal diameter of 48 mm and 70 cm in length. The fuel suspension was ignited by an electrically heated, 100-μm-diameter tungsten wire at the open end of the tube, with the flame propagating toward the closed end (dispersion system).

The fuel concentration in the suspension is controlled by varying the piston speed via an electromechanical linear actuator. The fuel concentration in the suspension can be calculated from the feeding rate of the piston, the packing density of the powder and the flow rate of the dispersing gas. The mass concentrations of iron powder varied in a range of 900-1,200 g/m^3.

The exhaust from the combustion tube is passed through a series of cooling and filtering systems and ultimately discharged into the aircraft cabin to accommodate the absence of overboard vents. The combustion products were drawn into the inlet of the cooling and filtering system by a vacuum blower. A wide annular opening between the combustion tube and the filtering system

(see Fig. 1, right bottom inset) ensures unobstructed access of the ambient air to maintain ambient pressure inside the combustion tube.

The combustion rack installed onboard the airplane contains four replaceable combustion tube assemblies (see Fig. 2). Each assembly is comprised of a combustion tube integrated with an individual powder dispersion unit. Four tube assemblies are mounted horizontally parallel to each other on the combustion rack, providing an unobstructed view for the optical diagnostics.

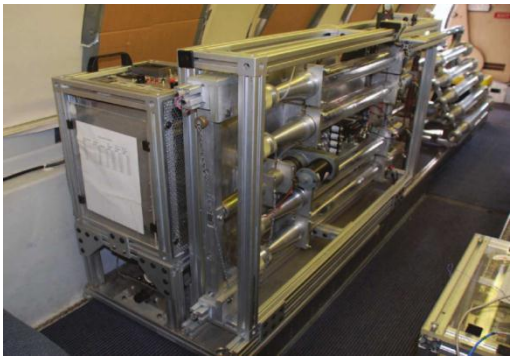

Figure 2: Photograph of the dust combustion apparatus installed on board parabolic flight aircraft.

The propagation of the flame was recorded by a high-speed digital camera viewing the entire length of the combustion tube at 300 frames per second.

The use of iron, that burns entirely in the condensed phase was motivated to ensure that the reaction occurred in the absence of the formation of vapors in the attempt to reflect the heterogeneous characteristics of the modeling. Five different iron powders were used in this investigation and are designated A to D in the Table I. Scanning electron microscope photographs of the iron powders are shown in Fig. 3.

Table I: Characteristics of iron powders used.

Powder	Particle shape	Purity	d_{10} (μm)	d_{32} (μm)
(a)	Spherical	99.9	3.3	4.3
(b)	Spherical	99.5	7.0	9.6
(c)	Spherical	99.5	9.9	13.7
(d)	Spherical	99.9	26.8	44.7

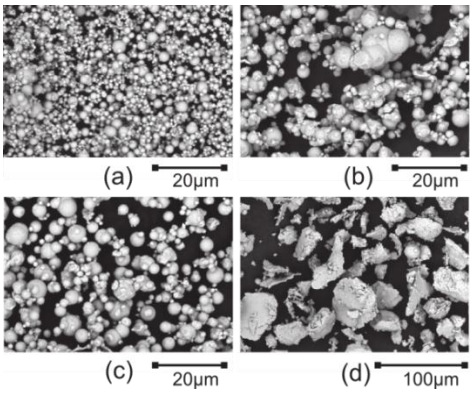

Figure 3: Scanning Electron Microscope (SEM) pictures of iron particles.

The experiments were performed using four separate gas mixtures containing helium or xenon at 21% and 40% oxygen concentration. The mixtures were supplied by a commercial gas supplier and were certified to be within an accuracy of 2%.

Results

The measured flame speeds from experiments performed in xenon and helium with 21% and 40% oxygen concentration are shown in Fig. 4. The flame speeds were obtained from the analysis of the high-speed videos. The error bar represents the standard deviation from 5 to 11 repeated measurements performed with the same gas mixture.

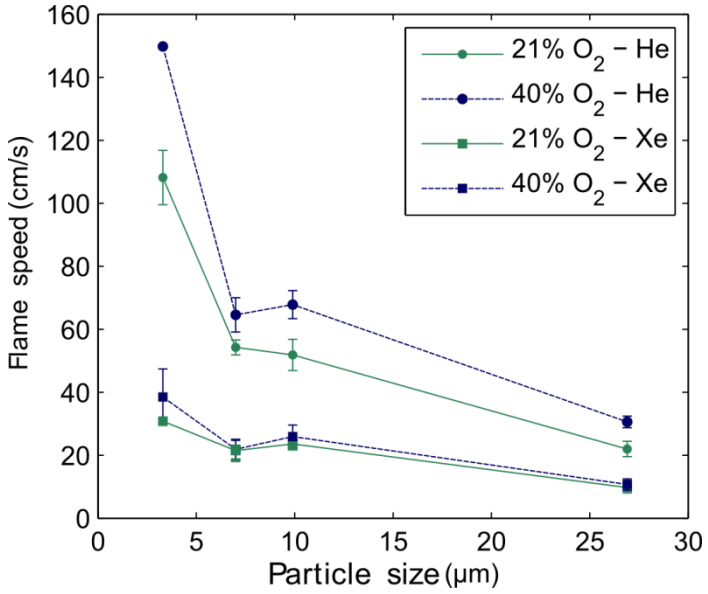

Figure 4: Flame speed measurements for iron powders A, B, C and D in He-O_2 and Xe-O_2 in 21% and 40% oxygen concentrations.

The flame speed is consistently larger in mixtures containing 40% compared to 21% oxygen. However, the difference is more pronounced in mixtures containing helium, compared to mixtures containing xenon.

Discussion

The ratios between the flame speeds in 40% and 21% oxygen concentration are shown in Fig. 5 for helium- and xenon-balanced mixtures and for the different particle sizes. The ratios corresponding to measurements performed in xenon mixtures are consistently lower than those for helium mixtures for all particle sizes. These measurements highlight the fact that flames propagating in xenon mixtures are less sensitive to variations of the oxygen concentration C_{O2} compared to flames in helium mixtures.

Using the shrinking core model of particle combustion, the oxygen concentration C_{O2} is related linearly to the particle combustion time t_r ($C_{O2} \sim t_r$) [6]. Hence, flame speeds measured in xenon mixtures are less sensitive to changes of the particle reaction time t_r compared to mixtures containing helium.

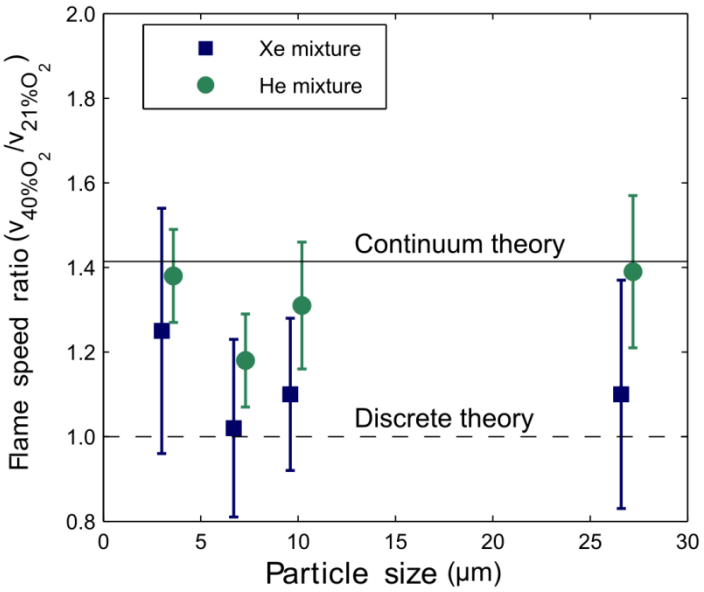

Figure 5: Ratio of the flame speeds between 21% and 40% O_2 in helium and xenon mixtures.

The stronger dependence of the flame speed on the reaction time t_r in mixtures containing helium compared to mixtures balanced with xenon can be attributed to a transition of the propagation regime from continuum to discrete. When substituting the balance inert gas from helium to xenon in 21% O_2, the dimensionless combustion time τ_c decreases from approximately 3.4 (continuum) to 0.6 (discrete).

Previous numerical work has shown that the discrete regime is characterized by a front speed that is independent of the reaction time t_r [7]. In other words, variations of the oxygen concentration do not affect the flame speed in the discrete regime. The flame speed ratio characteristic of the discrete regime reflects the insensitivity of the flame speed on the reaction time t_r:

$$\left.\frac{v_{40\%O_2}}{v_{21\%O_2}}\right|_{disc.} = 1. \qquad (2)$$

The distinctive relationship between the flame speed and the reaction time t_r in the discrete regime is in sharp contrast with the front speed predictions in a continuum. Using thermal theory, the flame speed v is expected to vary with the reaction time t_r as $v \sim 1/\sqrt{t_r}$ [8]. This behavior results in a ratio of the flame speeds $v_{40\%O_2}/v_{21\%O_2}$:

$$\left.\frac{v_{40\%O_2}}{v_{21\%O_2}}\right|_{cont.} = \sqrt{\frac{t_r(21\%)}{t_r(40\%)}} = \sqrt{\frac{40}{21}} \approx 1.4. \qquad (3)$$

In the discrete regime, the fact that flames exhibit a different behavior to change of the oxygen concentration from the predictions of the thermal theory highlights the breakdown of the continuum assumption. In the discrete regime, the heat release around particles becomes

localized to the point that the propagation of the flame becomes limited by the heat diffusion between neighboring particles. When the flame is controlled mainly by heat diffusion, the increase of the reaction rate of particles does not cause an increase of the flame speed.

In contrast, in a continuum, the limiting mechanism is assumed to be the particle reaction rate. This assumption underlines the fact that the reaction rate is treated as continuous function in space, where particles form a dense cloud of particles characterized by an interparticle spacing much smaller than the flame width.

Conclusion

The regime of propagation was investigated by varying the transport properties of the gas mixture as a means to change the dimensionless combustion time. Reduced experiments were performed in xenon- and helium-balanced mixtures to observe discrete and continuum flames, respectively. It was found that flames propagating in xenon-balanced mixtures were less sensitive to the oxygen concentration than flames propagating in helium-balanced mixtures. This observation reflects the distinct behavior of the flame propagation between the discrete and the continuum regimes.

Acknowledgement

This work was supported under Canadian Space Agency contract 9F007-052073/001/ST. The authors would like to thank the Flight Research Laboratory of the National Research Council of Canada.

References

1. K. Kleiner, "Powdered Metal: The Fuel of the Future," New Scientist, 2522 (2005), 34-
2. S. Goroshin, M. Bidabadi, J.H.S. Lee, "Quenching Distance of Laminar Flame in Aluminum Dust Clouds," Combustion and Flame, 105 (1996), 147-160.
3. A.G. Merzhanov, E.N. Rumanov, "Physics of Reaction Waves," Reviews of Modern Physics, 71 (1999), 1173-1211.
4. J.M. Beck, V. Volpert, "Nonlinear Dynamics in a Simple Model of Solid Flame Microstructure," Physica D, 182 (2003), 86-102.
5. S. Goroshin, J.H.S. Lee, Y. Shoshin, "Effect of the Discrete Nature of Heat Sources on Flame Propagation in Particulate Suspensions," Symposium (International) on Combustion, (27) 1998, 743-749.
6. J.C. Yang. "Heterogeneous Combustion," *Environmental Implications of Combustion Processes*, ed. I.K. Puri (Boca Raton, FL: CRC Press, 1993), 127-128.
7. S. Goroshin, F.D. Tang, A.J. Higgins, "Reaction-diffusion fronts in media with spatially discrete sources," Physical Review E, 84 (2011), 027301.
8. L.P Yarin and G. Hetsroni, *Combustion of Two-Phase Reactive Media* (Berlin: Springer-Verlag, 2004), 301.